ACS Combinatorial Science

Research Article

pubs.acs.org/acscombsci

Novel Use of Poly(3,4-ethylenedioxythiophene) Nanoparticles for Fluorescent Nucleic Acid Detection

Yingwei Zhang,[†] Sen Liu,[†] Lei Wang,[†] Yonglan Luo,[†] Jingqi Tian,[†,‡] Abdullah M. Asiri,[§,∥] Abdulrahman O. Al-Youbi,[§,∥] and Xuping Sun*[,†,§,∥]

[†]State Key Lab of Electroanalytical Chemistry, Changchun Institute of Applied Chemistry, Chinese Academy of Sciences, Changchun 130022, Jilin, China

[‡]Graduate School of the Chinese Academy of Sciences, Beijing 100039, China

[§]Chemistry Department, Faculty of Science, King Abdulaziz University, Jeddah 21589, Saudi Arabia

[∥]Center of Excellence for Advanced Materials Research, King Abdulaziz University, Jeddah 21589, Saudi Arabia

Supporting Information

ABSTRACT: In this paper, we demonstrate the novel use of poly(3,4-ethylene dioxythiophene) (PEDOT) nanoparticle as a very effective fluorescent sensing platform for the detection of nucleic acid sequences. The principle of the assay lies in the fact that the adsorption of the fluorescently labeled single-stranded DNA (ssDNA) probe by PEDOT nanoparticle leads to substantial fluorescence quenching, followed by specific hybridization with the complementary region of the target DNA sequence. This results in desorption of the hybridized complex from PEDOT nanoparticle surface and subsequent recovery of fluorescence. A detection limit as low as 30 pM could be achieved in this sensing system. We also demonstrate its application for multiplexed detection of nucleic acid sequences. Furthermore, this sensing system can realize the detection of single-base mismatch even in multiplexed format. It is of importance to note that the successful use of this sensing platform in human blood serum system is also demonstrated.

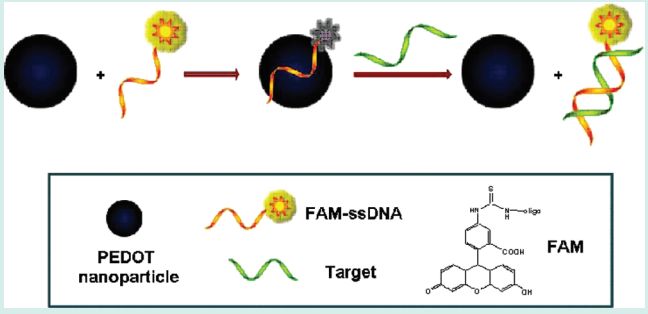

KEYWORDS: *poly(3,4-ethylenedioxythiophene), nanoparticles, fluorescent, nucleic acid detection, blood serum*

INTRODUCTION

In recent years, there has been growing interest in nucleic acid-based diagnostic tests because of their various applications in gene expression profiling, clinical disease diagnostics, and treatment. Therefore, it is vitally important to develop rapid, cost-effective, sensitive, and specific methods for the detection of nucleic acid.[1] The increasing availability of nanostructures has created widespread interest in their use in biotechnological system for diagnostic application.[2] Indeed, the use of a variety of nanostructures for this purpose has been well-documented.[3] Recently, there have been many efforts toward developing homogeneous fluorescence assays based on fluorescence resonance energy transfer (FRET) or quenching mechanism for nucleic acid detection.[4] It is a demonstrated fact using nanostructures as a "nanoquencher" has a remarkable advantage in that the same nanostructure has the ability to quench dyes of different emission frequencies and thus the selection issue of a fluorophore-quencher pair is eliminated from the nanostructure-involved system.[4,5] Up to now, many structures including gold nanoparticles, single-walled carbon nanotubes (SWCNTs) and graphene oxide (GO) have been used in this assay so far.[4−6] More recently, we have further demonstrated that other structures can also serve as an effective fluorescent sensing platform for DNA detection, including multiwalled carbon nanotubes, carbon nanoparticles (MWCNT), caobon nanospheres, nano-C_{60}, mesoporous carbon microparticles, poly(*p*-phenylenediamine) (PPPD) nanobelts, poly(*o*-phenylenediamine) (POPD) colloids, coordination polymer colloids and nanobelts and microdendrites, and porphyrin nanoparticles etc.[7]

On the other hand, conducting polymers have constituted a subject of research for their unique properties and important application potential during the past decades. Poly(3,4-ethylenedioxythiophene) (PEDOT) is one of the most promising conducting polymers and widely studied because it exhibits some very interesting properties including transparent in thin films, highly conductive, and more stable than most other conducting polymers;[8] however, its use for nucleic acid detection has never been addressed. In this paper, we report on the novel use of PEDOT nanoparticle as a very effective fluorescent sensing platform for multiplexed detection of nucleic acid sequences with a high selectivity down to single-

Received: August 24, 2011
Revised: December 1, 2011
Published: January 30, 2012

base mismatch for the first time. More importantly, the successful use of this sensing platform in human blood serum system is also demonstrated.

EXPERIMENTAL SECTION

All chemically synthesized oligonucleotides were purchased from Shanghai Sangon Biotechnology Co. Ltd. (Shanghai, China). DNA concentration was estimated by measuring the absorbance at 260 nm. All the other chemicals were purchased from Aladin Ltd. (Shanghai, China) and used as received without further purification. The water used throughout all experiments was purified through a Millipore system. PEDOT nanoparticles were prepared as follows: In a typical experiment, 0.5 mL of 0.2 M EDOT in tetrahydrofuran was prepared, then 0.5 mL of 1.6 M $FeCl_3$ aqueous solution was introduced, and the mix solution thus formed was heated at 80 °C for 4 h, leading to a deep green solution. The products were concentrated for 10 min at 12 000 rpm by centrifugating the solution and sequentially washed with 1 mL of water and ethanol several times to remove unused reactants and reaction byproducts and then were dispersed again in water for further characterization.

Scanning electron microscopy (SEM) measurements were made on a XL30 ESEM FEG scanning electron microscope at an accelerating voltage of 20 kV. Transmission electron microscopy (TEM) measurements were made on a HITACHI H-8100 EM (Hitachi, Tokyo, Japan) with an accelerating voltage of 100 kV. Zeta potential measurement was performed on a Nano-ZS Zetasizer ZEN3600 (Malvern Instruments Ltd., U.K.). Fluorescent emission spectra were recorded on a RF-5301PC spectrofluorometer (Shimadzu, Japan).

Fluorescent FAM, ROX, and Cy5 dyes are used to label oligonucleotide probes, and the core structures of these dyes are fluorescein, rhodamine, and cyanane, separately.[9] Oligonucleotide sequences are listed as follows (mismatch underlined):

(1) P_{HIV} (FAM dye-labeled ssDNA): 5′-FAM-AGT CAG TGT GGA AAA TCT CTA GC-3′
(2) T_0 (complementary target to P_{HIV}): 5′-GCT AGA GAT TTT CCA CAC TGA CT-3′
(3) T_1 (single-base mismatched target to P_{HIV}): 5′-GCT AGA GAT T<u>G</u>T CCA CAC TGA CT-3′
(4) T_2 (noncomplementary target to P_{HIV}): 5′-TTT TTT TTT TTT TTT TTT TT-3′
(5) P_{HBV} (ROX dye-labeled ssDNA): 5′-ROX-TAC CAC ATC ATC CAT ATA ACT GA-3′
(6) T_3 (complementary target to P_{HBV}): 5′-TCA GTT ATA TGG ATG ATG TGG TA-3′
(7) P_{K167} (Cy5 dye-labeled ssDNA): 5′-Cy5-TCT GCA CAC CTC TTG ACA CTC CG-3′
(8) T_4 (complementary target to P_{K167}): 5′-CGG AGT GTC AAG AGG TGT GCA GA-3′
(9) T_5 (single-base mismatched target to P_{HBV}): 5′-TCA GTT ATA <u>G</u>GG ATG ATG TGG TA-3′
(10) T_6 (single-base mismatched target to P_{K167}): 5′-TCT GCA CAC C<u>G</u>C TTG ACA CTC CG-3′
(11) T_{L1} (The middle part of a long strand as a target complementary to P_{HIV}): 5′-TTT TTT TTT TTT TTT TTT TGC TAG AGA TTT TCC ACA CTG ACT TTT TTT TTT TTT TTT TTT TTT T-3′
(12) T_{L2} (The middle part of a long strand as a single-base mismatched target to P_{HIV}): 5′-TTT TTT TTT TTT TTT TGC TAG AGA TT<u>G</u> TCC ACA CTG ACT TTT TTT TTT TTT TTT TTT TTT T-3′

In a typical DNA assay, the fluorescent probe P_{HIV} (50 nM) was prepared in Tris-HCl buffer (containing 20 mM Tris-HCl, 100 mM NaCl, 5 mM KCl, and 5 mM $MgCl_2$, pH 7.4). PEDOT nanoparticles were added into and the resultant mixture was incubated over a 1-h period, and then the fluorescence emission spectra were recorded on a RF-5301PC spectrofluorometer (Shimadzu, Japan). Target was then added into for hybridizing with probe and the fluorescence emission spectra were collected after incubation over a 1-h period. The experiments of multiplex detection were performed as follows: In a typical multiplex assay, P_{HIV}, P_{HBV}, and P_{K167} were added into Tris-HCl buffer to give a mixture of probes ($[P_{HIV}] = [P_{HBV}] = [P_{K167}] = 50$ nM). After that, PEDOT nanoparticles were added and the resultant mixture was incubated over a 1-h period, and then the fluorescence emission spectra were collected. Different target combinations were then added and the fluorescence emission spectra were collected after incubation over a 1-h period.

RESULTS AND DISCUSSION

Figure 1a shows typical SEM image of the products, indicating the formation of a large amount of agglomeration of

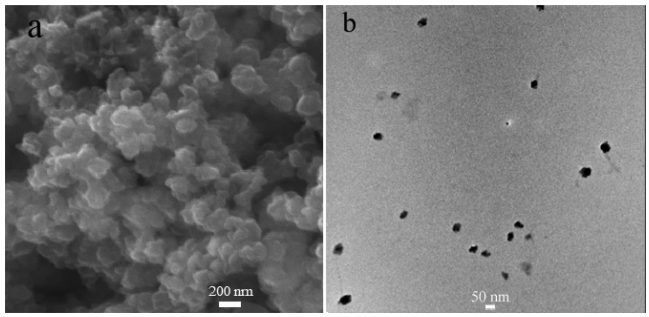

Figure 1. Typical SEM (a) and TEM (b) images of the PEDOT nanoparticles.

nanoparticles. Although these particles seem to have sintered, but the TEM image (Ethanol was used to disperse the PEDOT nanoparticles for TEM characterization.) shown in Figure 1b shows that these particles are not in direct physical contact and have diameters in the range of 20−45 nm. Supporting Information Figure S1 shows the size distribution histograms of such particles. We further examined the particle size in Tris-HCl buffer by dynamic light scattering (DLS) technique. The DSL results for the suspension reveal that the mean particle size of such dispersion is about 35 nm with narrow size distribution, which is in good agreement with the data obtained from TEM image. It should be mentioned that the obtained nanoparticles have a zeta potential of 2.71 mV and are well-dispersed in water. The chemical composition of the nanoparticles was determined by the energy dispersion spectrum (EDS), as shown in Supporting Information Figure S2. The peaks of C, O, and S elements are observed, indicating that the nanoparticles are formed from EDOT. The observation of the peak of C element can be attributed to the fact that the polymerization of EDOT by $FeCl_3$ yields positively charged PEDOT chains[10] and thus Cl^- as counterions diffuse into the PEDOT nanoparticles for charge compensation.

dx.doi.org/10.1021/co2001394 | ACS Comb. Sci. 2012, 14, 191−196

To test the feasibility of using PEDOT as an effective fluorescent sensing platform for nucleic acid detection, an oligonucleotide sequence associated with human immunodeficiency virus (HIV) is utilized as a model system. Figure 2 shows

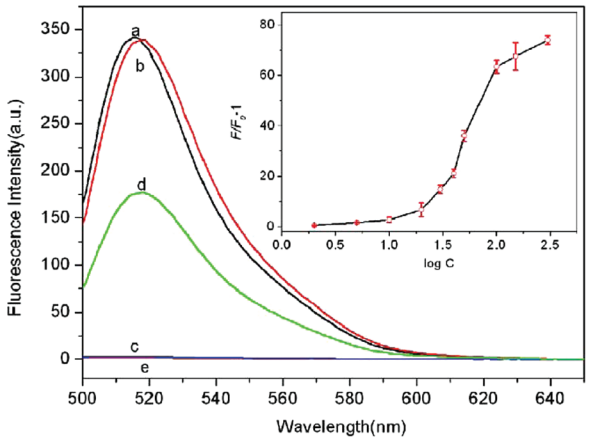

Figure 2. Fluorescence emission spectra of P_{HIV} (50 nM) at different conditions: (a) P_{HIV}; (b) P_{HIV} + 300 nM T_0; (c) P_{HIV} + PEDOT nanoparticles; (d) P_{HIV} + PEDOT nanoparticles +300 nM T_0. Curve e is the emission spectra of PEDOT nanoparticle. Inset: fluorescence intensity ratio of P_{HIV}–PEDOT nanoparticle complex with $F/F_0 - 1$ (where F_0 and F are the fluorescence intensity without and with the presence of T_0, respectively) plotted against the logarithm of the concentration of T_0. Excitation was at 480 nm, and the emission was monitored at 518 nm. All measurements were done in Tris-HCl buffer in the presence of 5 mM Mg^{2+} (pH 7.4).

the fluorescence emission spectra (excitation at 480 nm) of P_{HIV}, the FAM-labeled probe, at different conditions. In the absence of PEDOT, the fluorescence spectrum of P_{HIV} exhibits strong fluorescence emission due to the presence of the fluorescein-based dye (curve a). However, the presence of PEDOT results in about 99% quenching of the fluorescence emission (curve c), revealing the nanoparticles can strongly adsorb ssDNA and quench the fluorescent dye very effectively. It should be mentioned that the quenching efficiency of the PEDOT nanoparticles is higher than that of the other systems, such as SWCNT, GO, MWCNT, caobon nanospheres, nano-C_{60}, mesoporous carbon microparticles, PPPD nanobelts, POPD colloids, coordination polymer colloids and nanobelts and microdendrites, and porphyrin nanoparticles.[6f–h,7] The P_{HIV}-PEDOT complex exhibits significant fluorescence enhancement upon its incubation with complementary target T_0 over a 1-h period, leading to a 52% fluorescence recovery (curve d). The fluorescence enhancement was caused by the release of dsDNA from PEDOT, which is supported by the following experimental observation that there is no obvious fluorescence change observed after the removal of the PEDOT from the solution by centrifugation (Supporting Information Figure S3). Note that the fluorescence of the free P_{HIV} was, however, scarcely influenced by the addition of T_0 in the absence of PEDOT (curve b). Figure 2 inset illustrates the fluorescence intensity changes of P_{HIV}–PEDOT complex upon addition of different concentrations of T_0, where F_0 and F are FAM fluorescence intensities at 518 nm in the absence and the presence of T_0, respectively. In the DNA concentration range of 20–300 nM, a dramatic increase of FAM fluorescence intensity was observed, which suggests that the nanoparticle/DNA assembly approach is effective in probing biomolecular interactions because of the excellent signaling process. The observation that target concentration needs to reach some threshold level to yield fluorescence enhanced could be explained as follows: the PEDOT nanoparticle surface cannot be completely covered by the probes, leading to direct adsorption of some targets on its surface instead of hybridization with preadsorbed probes. As a result, enough targets must be present to give observable fluorescence enhancement. It is of importance to note that a detection limit of 30 pM was achieved when the experiment was carried out using 10-μL PEDOT and 500 pM P_{HIV} (Supporting Information Figure S4), which is lower than that of previous reported 4.0 nM of SWCNT and 2.0 nM of GO. Also note that the PEDOT sample exhibits extremely weak fluorescence emission (curve e) which contributes little to the whole fluorescence intensity of each sample measured.

PEDOT is a π-rich structure and thus there should be strong $\pi-\pi$ stacking interactions between ssDNA bases and PEDOT,[11] leading to strong adsorption of ssDNA on PEDOT. The zeta potential of the nanoparticles was measured to be about 2.71 mV, indicating that the PEDOT has a low positively charged surface. So, the slight electrostatic attractive interactions between PEDOT and negatively charged backbone of ssDNA only contribute little to the adsorption of ssDNA on PEDOT. In contrast, PEDOT should have weak or no binding with dsDNA due to the absence of unparied DNA bases and the rigid conformation of dsDNA. Scheme 1 shows a schematic to illustrate the PEDOT-based fluorescent nucleic acid

Scheme 1. Fluorescence-Enhanced Nucleic Acid Detection Using PEDOT Nanoparticle As a Sensing Platform (Not to Scale)

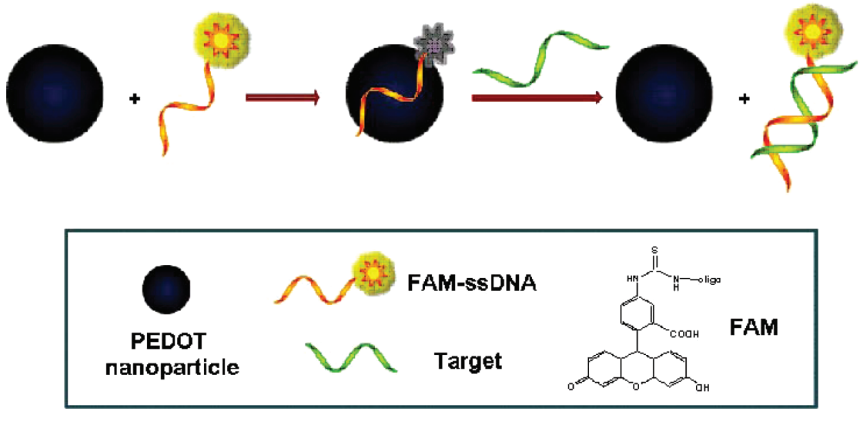

dx.doi.org/10.1021/co2001394 | ACS Comb. Sci. 2012, 14, 191–196

detection mechanism. The DNA detection is accomplished by the following two steps: (1) PEDOT binds FAM-ssDNA via both electrostatic attraction and $\pi-\pi$ stacking interactions between DNA bases and PEDOT. As a result, substantial fluorescence quenching of the dye occurs due to their close proximity; (2) the hybridization of FAM-ssDNA with its target leads to a dsDNA which detaches and thus liberates FAM-ssDNA from PEDOT, leading to fluorescence recovery.

It is worthwhile mentioning that the sensing platform described herein can differentiate complementary and mismatched sequences. Figure 3 shows the fluorescence responses

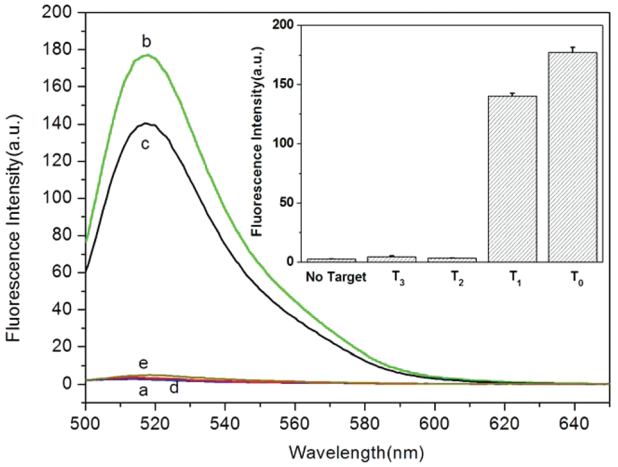

Figure 3. Fluorescence emission spectra of P_{HIV} (50 nM) at different conditions: (a) P_{HIV}-PEDOT complex; (b) P_{HIV}-PEDOT complex +300 nM T_0; (c) P_{HIV}-PEDOT complex +300 nM T_1; (d) P_{HIV}-PEDOT complex +300 nM T_2; (e) P_{HIV}-PEDOT complex +300 nM T_3. Inset: Fluorescence intensity histograms with error bar. Excitation was at 480 nm, and the emission was monitored at 518 nm. All measurements were done in Tris-HCl buffer in the presence of 5 mM Mg^{2+} (pH 7.4).

of P_{HIV}-PEDOT complex toward complementary target T_0, and single-base mismatched target T_1, respectively. The F/F_0 value obtained upon addition of 300 nM of T_1 is about 79% of the value obtained upon addition of 300 nM of T_0 into P_{HIV}-PEDOT complex, indicating the selectivity of the present system is down to single-base mismatch. Furthermore, we performed the control experiments where two noncomplementary targets to P_{HIV} (T_2 and T_3) were added into P_{HIV}-PEDOT complex respectively, but failed to observe any fluorescence recovery (curve d and e). Such observation verifies that the observed fluorescence enhancement in our present system is indeed due to the base pairing between probe and its complementary target detected. Compared to the complementary target, the mismatched target should have lower hybridization ability toward the adsorbed dye-labeled ssDNA probe, leading to a decreased hybridization and thus fluorescence recovery efficiency. The inset is the corresponding fluorescence intensity histograms with error bar.

We further evaluated its ability of this sensing platform to distinguish single-base mismatch by mimicking the realistic situations, where a short oligonucleotide probe binds a small loci of a large DNA strand. Two long DNA strands were chosen as model systems: the middle part of T_{L1} is complementary target sequence to P_{HIV} and the middle part of T_{L2} is single-base-mismatched target sequence to P_{HIV}. Figure 4 shows the fluorescence responses of P_{HIV} toward T_{L1}

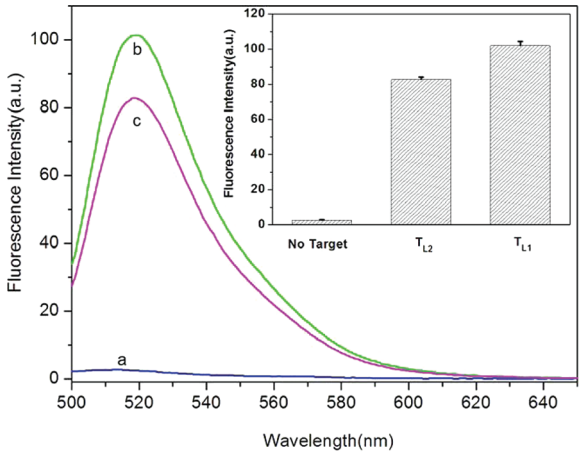

Figure 4. Fluorescence emission spectra of P_{HIV} (50 nM) at different conditions: (a) P_{HIV}-PEDOT complex; (b) P_{HIV}-PEDOT complex + 300 nM T_{L1}; (c) P_{HIV}-PEDOT complex + 300 nM T_{L2}. Inset: Fluorescence intensity histograms with error bar.

and T_{L2} in the presence of PEDOT at room temperature. The addition of 300 nM of T_{L1} to P_{HIV}–PEDOT complex leads to about 30% fluorescence recovery which is much lower than 52% observed when 300 nM of T_1 was used as the target. Such observation is not surprising given that P_{HIV}–T_{L1} is a complex with a duplex DNA in the middle and two single strands on both ends and thus there are unpaired DNA bases for binding to PEDOT. The F/F_0 value obtained upon addition of 300 nM of T_{L2} is about 80% of the value obtained upon addition of 300 nM of T_{L1} into P_{HIV}–PEDOT complex, indicating that this sensing platform is still able to discriminate complementary and mismatched target sequences embedded in a large DNA strand with a short oligonucleotide probe. All the above observations suggest that the present sensing system has a high selectivity down to single-base mismatch and the results exhibit good reproducibility, and therefore, hold great promise for single-nucleotide polymorphism detection application.

We also performed DNA detection in human blood serum. Figure 5 shows the fluorescence emission spectra of P_{HIV} in the presence of 20% blood serum (volume ratio) in Tris-HCl buffer at different conditions. This system exhibits 92% fluorescence quenching and 38% fluorescence recovery and the difference of detection signal between single-base mismatched and complementary sequences is 79%. All the above observations indicate that there is no heavy interference from blood serum components on our measurements and thus this sensing system is promising for practically useful mismatch detection upon further development.

Multiplexed detection of nucleic acid sequences is challenging for many assays because of the need of eliminating probe set/target set cross-reactivity, minimizing nonspecific binding, and designing spectroscopically and chemically unique probes,[12] which motived us to explore the feasibility of using the platform described herein to detect multiple DNA targets simultaneously. To do this, we choose three probes (P_{HIV}, P_{HBV}, and P_{K167}) labeled with FAM, ROX, and Cy5 (cyanine 5), respectively, as model systems. Because these three dyes were individually excited at 480, 587, and 643 nm to emit at 522, 601, and 660 nm, respectively, significant dye-to-dye energy transfer is avoided. It is found that the presence of PEDOT leads to dramatic quenching of all dyes in the probe mixture, indicating that PEDOT can effectively quench dyes of different

dx.doi.org/10.1021/co2001394 | ACS Comb. Sci. 2012, 14, 191–196

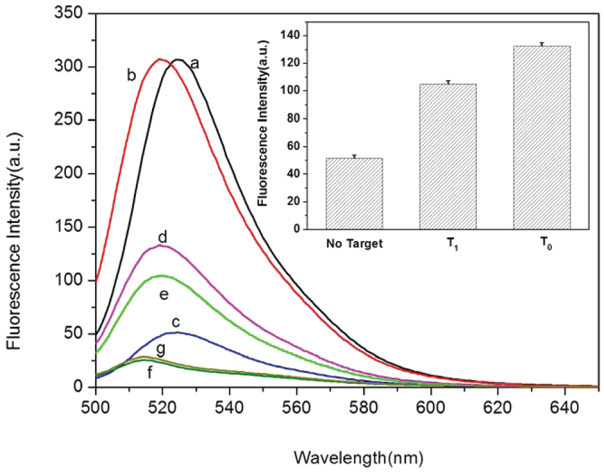

Figure 5. Fluorescence emission spectra of P_{HIV} (50 nM) at different conditions: (a) P_{HIV}; (b) P_{HIV} + 300 nM T_0; (c) P_{HIV}-PEDOT complex; (d) P_{HIV}-PEDOT complex +300 nM T_0; (e) P_{HIV}-PEDOT complex +300 nM T_1 . Curve f and g are the emission spectra of PEDOT nanoparticle and Tris-HCl buffer in the presence of 20% (volume ratio) human blood serum. Inset: fluorescence intensity histograms with error bar. All measurements were done in Tris-HCl buffer (pH 7.4) containing 20% (volume ratio) human blood serum and 5 mM Mg^{2+} at room temperature.

emission frequencies. Figure 6 shows the fluorescence intensity histograms of the probe mixture toward different target

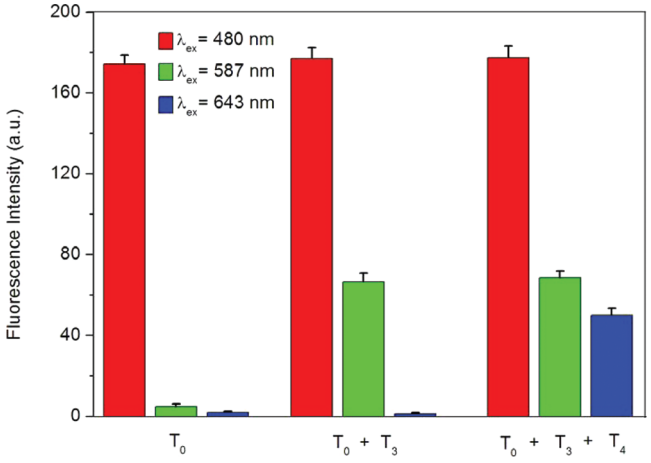

Figure 6. Fluorescence intensity histograms of the probe mixture ($[P_{HIV}]$ = $[P_{HBV}]$ = $[P_{K167}]$ = 50 nM) toward different target combinations in the presence of PEDOT under excitation/emission wavelengths of 480/522, 587/601, and 643/660 nm/nm ($[T_0]$ = $[T_3]$ = $[T_4]$ = 300 nM). All measurements were done in Tris-HCl buffer in the presence of 5 mM Mg^{2+} (pH 7.4).

combinations ($[T_0]$ = $[T_3]$ = $[T_4]$ = 300 nM) in the presence of PEDOT under excitation/emission wavelengths of 480/522, 587/601, and 643/660 nm/nm. It is clearly seen that there is only one strong emission peak at 522 nm when excited by 480 nm in the presence of T_0 only. However, the target combination of T_0 + T_3 gives two strong emission peaks at 522 and 601 nm when excited by 480 and 587 nm, respectively. As expected, three strong emission peaks are observed for the T_0 + T_3 + T_4 target combination at 522, 601, and 660 nm when excited by 480, 587, and 643 nm, respectively.

We also performed multiplexed detection at lower target concentration of 50 nM successfully, as shown in Supporting Information Figure S5, indicating that lower concentration of target in the mixture leads to decreased fluorescence enhancement. Supporting Information Figure S6 shows the fluorescence intensity histograms of the probe mixture ($[P_{HIV}]$ = $[P_{HBV}]$ = $[P_{K167}]$ = 50 nM) toward different single-base mismatched target combinations in the presence of PEDOT under excitation/emission wavelengths of 480/522, 587/601, and 643/660 nm/nm($[T_1]$ = $[T_5]$ = $[T_6]$ = 300 nM). Compared with complementary target combinations (Figure 6), the mismatched target combinations lead to obviously decreased fluorescence recovery. It suggests that this system can be used in a multiplexed format to detect single-base mismatches. All these observations indicate that this sensing platform can be used to detect multiple DNA targets with high selectivity. It is of importance to note that, although fluorescence-based multiplexed is limited to different wavelength ranges, the use of two or three (even more) dyes labeled DNA probes makes this detection technique more multiplexed with an additional advantage of simultaneous detection of multiple targets with single excitation based on FRET between these dyes. Thus, our detection technique could find a unique niche in a broad perspective.

It should be noted that the amount of PEDOT nanoparticles used in this system has profound effect on the efficiency of the fluorescence quenching and the subsequent recovery as well. Figure 7 shows the fluorescence intensity histograms of five

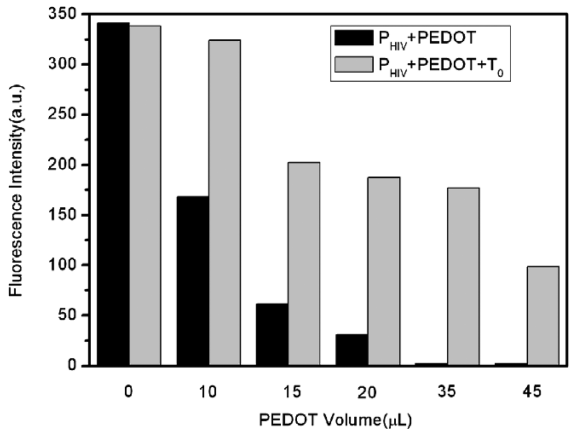

Figure 7. Fluorescence intensity histograms of P_{HIV} + PEDOT and P_{HIV} + PEDOT + T_0 with the using of 0, 10, 15, 20, 35, and 45-μL PEDOT sample in this system ($[P_{HIV}]$ = 50 nM; $[T_0]$ = 300 nM; λ_{ex} = 480 nm).

samples with the use of 0, 10, 15, 20, 35, and 45-μL PEDOT nanoparticles sample, respectively, suggesting that the use of increased amount of nanoparticles leads to an increase in quenching efficiency but a decrease in recovery efficiency. The above observations can be reasoned as follows: When the ssDNA probe molecules are mixed with nanoparticles, they will adsorb on the nanoparticle surface. Obviously, the use of more nanoparticles leads to more efficient adsorption of ssDNA and thus higher quenching efficiency, but at the same time, the possibility of direct surface adsorption of target molecules on those excess nanoparticles increases during the following hybridization process. As a result, decreased hybridization efficiency and thus lower recovery efficiency are observed.

dx.doi.org/10.1021/co2001394 | ACS Comb. Sci. 2012, 14, 191–196

Based on these observations, a 35-μL PEDOT sample was chosen in our present study.

CONCLUSIONS

In summary, we demonstrate the novel use of PEDOT nanoparticles as a very effective sensing platform for fluorescence-enhanced, multiplex nucleic acid detection with selectivity down to single-base mismatch for the first time. Our present observations are significant for the following two reasons: (1) It extends the application of PEDOT to nucleic acid detection; (2) This sensing platform is promising for universal and effective fluorescence-enhanced detection sensitive and selective to the target molecule studied.

ASSOCIATED CONTENT

Supporting Information

EDS, fluorescence spectra, and fluorescence intensity histograms. This material is available free of charge via the Internet at http://pubs.acs.org.

AUTHOR INFORMATION

Corresponding Author

*Tel/Fax: 0086-431-85262065. E-mail: sunxp@ciac.jl.cn.

ACKNOWLEDGMENTS

This work was supported by the National Natural Science Foundation of China (No. 21175129) and the National Basic Research Program of China (No. 2011CB935800).

REFERENCES

(1) Gresham, D.; Ruderfer, D. M.; Pratt, S. C.; Schacherer, J.; Dunham, M. J.; Botstein, D.; Kruglyak, L. Genome-wide detection of polymorphisms at nucleotide resolution with a single DNA microarray. *Science* **2006**, *311*, 1932−1936.

(2) Brayner, R. The toxilogical impact of nanoparticles. *Nanotoday* **2008**, *3*, 48−55.

(3) Rosi, N. L.; Mirkin, C. A. Nanostructures in biodiagnostics. *Chem. Rev.* **2005**, *105*, 1547−1562.

(4) Ray, P. C.; Darbha, G. K.; Ray, A.; Walker, J.; Hardy, W. Gold nanoparticle based FRET for DNA detection. *Plasmonics* **2007**, *2*, 173−183.

(5) Yang, R.; Tang, Z.; Yan, J.; Kang, H.; Kim, Y.; Zhu, Z.; Tan, W. Noncovalent assembly of carbon nanotubes and single-stranded DNA: An effective sensing platform for probing biomolecular interactions. *Anal. Chem.* **2008**, *80*, 7408−7413.

(6) (a) Dubertret, B.; Calame, M.; Libchaber, A. Single-mismatch detection using gold-quenched fluorescent oligonucleotides. J. *Nat. Biotechnol.* **2001**, *19*, 365−370. (b) Maxwell, D. J.; Taylor, J. R.; Nie, S. Self-assembled nanoparticle probes for recognition and detection of biomolecules. *J. Am. Chem. Soc.* **2002**, *124*, 9606−9612. (c) Li, H.; Rothberg, L. DNA sequence detection using selective fluorescence quenching of tagged oligonucleotide probes by gold nanoparticles. *J. Anal. Chem.* **2004**, *76*, 5414−5417. (d) Song, S.; Liang, Z.; Zhang, J.; Wang, L.; Li, G.; Fan, C. Gold-nanoparticle-based multicolor nanobeacons for sequence-specific DNA analysis. *Angew. Chem., Int. Ed.* **2009**, *48*, 8670−8674. (e) Li, D.; Song, S.; Fan, C. Target-responsive structural switching for nucleic acid-based sensors. *Acc. Chem. Res.* **2010**, *43*, 631−641. (f) Yang, R.; Jin, J.; Chen, Y.; Shao, N.; Kang, H.; Xiao, Z.; Tang, Z.; Wu, Y.; Zhu, Z.; Tan, W. Carbon nanotube-quenched fluorescent oligonucleotides: Probes that fluoresce upon hybridization. *J. Am. Chem. Soc.* **2008**, *130*, 8351−8358. (g) Lu, C.; Yang, H.; Zhu, C.; Chen, X.; Chen, G. A graphene platform for sensing biomolecules. *Angew. Chem., Int. Ed.* **2009**, *48*, 4785−4787. (h) He, S.; Song, B.; Li, D.; Zhu, C.; Qi, W.; Wen, W.; Wang, L.; Song, S.; Fang, H.; Fan, C. A graphene nanoprobe for rapid, sensitive, and multicolor fluorescent DNA analysis. *Adv. Funct. Mater.* **2010**, *20*, 453−459.

(7) (a) Li, H.; Tian, J.; Wang, L.; Zhang, Y.; Sun, X. Multi-walled carbon nanotubes as an effective fluorescent sensing platform for nucleic acid detection. *J. Mater. Chem.* **2011**, *21*, 824−828. (b) Li, H.; Zhang, Y.; Wang, L.; Tian, J.; Sun, X. Nucleic acid detection using carbon nanoparticles as an fluorescent sensing platform. *Chem. Communu.* **2011**, *47*, 961−963. (c) Li, H.; Zhang, Y.; Wu, T.; Liu, S.; Wang, L.; Sun, X. Carbon nanospheres for fluorescent biomolecular detection. *J. Mater. Chem.* **2011**, *21*, 4663−4668. (d) Li, H.; Zhang, Y.; Luo, Y.; Sun, X. Nano-C_{60}: A novel, effective fluorescent sensing platform for biomolecular detection. *Small* **2011**, *7*, 1562−1568. (e) Liu, S.; Li, H.; Wang, L.; Tian, J.; Sun, X. New application of mesoporous carbon microparticles to nucleic acid detection. *J. Mater. Chem.* **2011**, *21*, 339−341. (f) Wang, L.; Zhang, Y.; Tian, J.; Li, H.; Sun, X. Conjugation polymer nanobelts: A novel fluorescent sensing platform for nucleic acid detection. *Nucleic Acids Res.* **2011**, *39*, e37−e42. (g) Tian, J.; Li, H.; Luo, Y.; Wang, L.; Zhang, Y.; Sun, X. Poly(*o*-phenylenediamine) colloid-quenched fluorescent oligonucleotide as a probe for fluorescence-enhanced nucleic acid detection. *Langmuir* **2011**, *27*, 874−877. (h) Li, H.; Sun, X. Fluorescence-enhanced nucleic acid detection: Using coordination polymer colloids as a sensing platform. *Chem. Commun.* **2011**, *47*, 2625−2627. (i) Li, H.; Wang, L.; Zhang, Y.; Tian, J.; Sun, X. Coordination polymer nanobelts as an effective sensing platform for fluorescence-enhanced nucleic acid detection. *Macromol. Rapid Commun.* **2011**, *32*, 899−904. (j) Li, H.; Zhai, J.; Sun, X. Large-scale synthesis of coordination polymer microdendrites and their application as a sensing platform for fluorescent DNA detection. *RSC Adv.* **2011**, *1*, 725−730. (k) Zhai, J.; Li, H.; Sun, X. A novel application of porphyrin nanoparticles as an effective fluorescent assay platform for nucleic acid detection. *RSC Adv.* **2011**, *1*, 36−39.

(8) Groenendaal, L. B.; Jonas, F.; Freitag, D.; Pielartzik, H.; Reynolds, J. R. Poly(3,4-ethylenedioxythiophene) and its derivatives: Past, present, and future. *Adv. Mater.* **2000**, *12*, 481−494.

(9) Didenko, V. V. *Fluorescent Energy Transfer Nucleic Acid Probes*; Humana Press: Totowa, NJ, 2006; Part II.

(10) Sun, X.; Hagner, M. Mixing aqueous ferric chloride and *o*-phenylenediamine solutions at room temperature: A fast, economical route to ultralong microfibrils of assemblied *o*-phenylenediamine dimmers. *Macromolecules* **2007**, *40*, 8537−8539.

(11) Varghese, N.; Mogera, U.; Govindaraj, A.; Das, A.; Maiti, P. K.; Sood, A. K.; Rao, C. N. R. Binding of DNA nucleobases and nucleosides with graphene. *ChemPhysChem* **2009**, *10*, 206−210.

(12) Stoeva, S. I.; Lee, J.-S.; Thaxton, C. S.; Mirkin, C. A. Multiplexed DNA detection with biobarcoded nanoparticle probes. *Angew. Chem., Int. Ed.* **2006**, *45*, 3303−3306.